



## INTERNATIONAL JOURNAL OF ENGINEERING SCIENCES & RESEARCH TECHNOLOGY

### PERFORMANCE EVALUATION OF MULTIBAND OFDM FOR UWB AND ZIGBEE COMMUNICATIONS

N.Dhasarathan Alias Raja\*, P.C.Agarawal

\* Research Scholar, 2Faculty Member, Dept of ECE, Bundelkhand University, U.P., India

Research Scholar, 2Faculty Member, Dept of ECE, Bundelkhand University, U.P., India

---

#### ABSTRACT

In this paper, we analyze the Multiband orthogonal frequency-division multiplexing (OFDM) system for high-rate wireless personal area networks (WPANs) based on ultra-wideband (UWB) transmission and with the help of Zigbee transceiver. We also propose system performance through the application of Turbo and Repeat-Accumulate (RA) codes. Our methodology consists of (c) simulation results for the Multiband OFDM standard proposal as well as our proposed extensions, and (d) the consideration of the influence of practical, imperfect channel estimation on the performance. We find that the current Multiband OFDM standard sufficiently exploits the frequency selectivity of the UWB channel. Reduced-complexity clustered bit-loading algorithm improves the system power efficiency by over 6 dB at a data rate of 480 Mbps. Also in this paper we have tried to improve Error rate performance of Zigbee Personal Area Network (PAN) using multiple transmitters on existing system with OQPSK modulation in AWGN channel environment. From the simulation results we have found that our proposed multiple transmitters scheme (MISO) gives quite better results on low SNR values comparatively with the existing Single Input Single Output (SISO) approach.

**KEYWORDS:** Ultra wideband, Multiband OFDM, MISO, ZIGBEE, OQPSK.

---

#### INTRODUCTION

Ultra-wideband (UWB) radio has recently been popularized as a technology for short-range, high data rate communication and locationing applications. The IEEE 802.15 standardization group, responsible for wireless personal area networks (WPANs), organized task group 3a to develop an alternative physical layer based on UWB signaling. There were two main contenders for this standard: a frequency hopping orthogonal frequency-division multiplexing (OFDM) proposal known as Multiband OFDM and a code-division multiple access (CDMA) based technique. In this paper, we consider the proposed Multiband OFDM standard. Multiband OFDM is a conventional OFDM system combined with bit-interleaved coded modulation (BICM) for error prevention and frequency hopping for multiple access and improved diversity. The signal bandwidth is 528 MHz, which makes it a UWB signal according to the definition of the US Federal Communications Commission (FCC), and hopping between three adjacent frequency bands is employed for first generation devices. Thus, the Multiband OFDM proposal is a rather pragmatic approach for UWB transmission, which builds upon the proven BICM-OFDM concept. The objective of this paper is to analyze the performance of Multiband

OFDM for UWB transmission. Furthermore, we propose system performance enhancements by applying capacity-approaching Turbo and Repeat-Accumulate (RA) codes and by using OFDM bit loading. These specific techniques were chosen because of their potential for improved system performance without requiring substantial changes to other portions of the Multiband OFDM system, nor requiring major increases in complexity. Since our investigations rely on the new UWB channel model developed under IEEE 802.15, we first analyze this channel model in the frequency domain and extract the relevant statistical parameters that affect the performance of OFDM based transmission. In particular, the amount of diversity available in the wireless channel as a function of the signal bandwidth is examined. As appropriate performance measures for coded communication systems, we discuss the capacity and cutoff rate limits of BICM-OFDM systems for UWB channels. In this context, since one limiting factor of performance in practical and especially in wideband BICM-OFDM systems is the availability of high-quality channel state estimates, the effect of imperfect channel state information (CSI) at the receiver is specifically addressed. Furthermore, the information-theoretic performance limits are

compared with simulated bit-error rate (BER) results. An extension to the standard proposal, simplified Low-Density Parity-Check (LDPC) codes are considered in order to improve the power efficiency of the Multiband OFDM system for a subset of the proposed data rates. A sub band and power allocation strategy for a multiuser Multiband OFDM system is given in [1], but each user in the system uses a fixed modulation (i.e. no per-user bit allocation is performed).

ZigBee is a specification for a suite of high level communication protocols based on the IEEE 802.15.4 physical and MAC layers. The specification is developed by a group of industry players, the ZigBee Alliance. Some of the commercial applications of WSNs using ZigBee are in the area of home and building automation, remote control or health care monitoring. IEEE 802.15.4 Standard provides for very low complexity, very low cost, very low power consumption, and low data rate wireless connectivity among low-cost devices. The data rate is high enough (250 kb/s) to meet a set of applications but is also scalable down to the needs of sensor and automation requirements (20 kb/s or below) for wireless communications. In addition, one of the alternate PHYs provides precision ranging capability that is accurate to one meter. Multiple PHYs are defined to support various frequency bands including

- i. 868–868.6 MHz
- ii. 902–928 MHz
- iii. 2400–2483.5 MHz
- iv. 314–316 MHz, 430–434 MHz, and 779–787 MHz band for LR-WPAN systems in China
- v. 950–956 MHz in Japan.

The major standardization bodies in the WSN area are the Institute of Electrical and Electronics Engineers (IEEE), the Internet Engineering Task Force (IETF) and the HART communication foundation. Notable standards and specifications are:

#### IEEE 802.15.4 Standard

This standard [4] specifies the PHY and MAC layer for low-rate WPANs. Many platforms are based on this standard and other specifications, such as ZigBee and wireless HART specifications, are built on top of the standard covering the upper layers to provide a complete networking solution. Some of the main characteristics of the IEEE 802.15.4 are:

- 250 kbps, 40 kbps and 20 kbps data rates.
- Two addressing modes, 16-bit short and 64-bit IEEE addressing.
- CSMA-CA channel access.

- Automatic network establishment by the coordinator of the network.
- Power management control.
- 16 channels in the 2.4 GHz ISM band, 10 channels in the 915 MHz ISM band and one channel in the 868 MHz band.

#### Major Parts of the IEEE 802.15.4 WPAN

A system meeting the requirements to this standard consists of several components. The most basic is the device. Two or more devices communicating on the same physical channel constitute a WPAN. However, this WPAN includes at least one FFD, which operates as the PAN coordinator.[2]

#### UWB CHANNEL MODEL

For a meaningful performance analysis of the Multiband OFDM proposal, we consider the channel model developed under IEEE 802.15 for UWB systems [3]. The channel impulse response is a Saleh-Valenzuela model [4] modified to fit the properties of measured UWB channels. Multipath rays arrive in clusters with exponentially distributed cluster and rays inter arrival times. Both clusters and rays have decay factors chosen to meet a given power decay profile. The ray amplitudes are modeled as lognormal random variables, and each cluster of rays also undergoes a lognormal fading. To provide a fair system comparison, the total multipath energy is normalized to unity. Finally, the entire impulse response undergoes an “outer” lognormal shadowing. The channel impulse response is assumed time invariant during the transmission period of several packets [3]. Four separate channel models (CM1-CM4) are available for UWB system modeling, each with arrival rates and decay factors chosen to match a different usage scenario. The four models are tuned to fit 0-4 m Line-of-Sight (LOS), 0-4 m non-LOS, 4-10 m non-LOS, and an “extreme non-LOS multipath channel”, respectively. The means and standard deviations of the outer lognormal shadowing are the same for all four models [3].

#### Diversity Combining, Demapping, and Decoding

Maximum-ratio combining (MRC) [5] in the case of time and/or frequency spreading and demapping in the standard BICM fashion [6] are performed based on the channel estimator output  $\hat{H}$ . The resulting “soft” bit metrics are deinterleaved and depunctured. Convolutionally coded schemes use a soft-input Viterbi decoder to restore the original bit stream, requiring a decoding complexity of 64 trellis states searched per information bit. Turbo-coded schemes are decoded with 10 iterations of a conventional Turbo

decoder using the log-domain BCJR algorithm [7], with a complexity of roughly  $10 \cdot 2 \cdot 2 \cdot 8 = 320$  trellis states searched per information bit (i.e. 10 iterations of two 8-state component codes, and assuming that the BCJR algorithm is roughly twice as complex as the Viterbi algorithm due to the forward-backward recursion). RA decoding is performed by a turbo-like iterative decoder, using a maximum of 60 iterations and an early-exit criterion which, at relevant values of SNR, reduces the average number of decoder iterations to less than ten [8]. We note that the periteration decoding complexity of the RA code is less than that of the Turbo code (since only a 2-state accumulator and a repetition code are used), making the total RA decoder complexity slightly more than the convolutional code but less than the Turbo code.

### Zigbee frame structure

The super frame is defined between two beacon frames and has an active period and an inactive period. The active portion of the super frame structure is composed of three parts, the Beacon, the Contention Access Period (CAP) and the Contention Free Period (CFP):

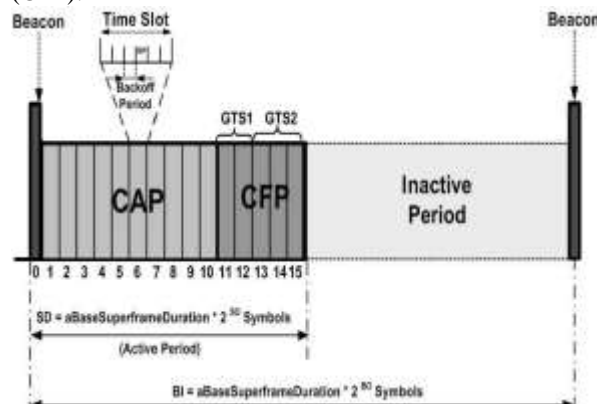


Figure 1 - IEEE 802.15.4 Super frame Structure

**Beacon:** The beacon frame is transmitted at the start of slot 0. It contains the information on the addressing fields, the super frame specification, the GTS fields, the pending address fields and other PAN related.

**Contention Access Period (CAP):** The CAP starts immediately after the beacon frame and ends before the beginning of the CFP, if it exists. Otherwise, the CAP ends at the end of the active part of the super frame. The minimum length of the CAP is fixed at  $aMinCAPLength = 440$  symbols. This minimum length ensures that MAC commands can still be transmitted when GTSs are being used. A temporary violation of this minimum may be allowed if additional space is needed to temporarily

accommodate an increase in the beacon frame length, needed to perform GTS management. All transmissions during the CAP are made using the Slotted CSMA/CA mechanism. However, the acknowledgement frames and any data that immediately follows the acknowledgement of a data request command are transmitted without contention. If a transmission cannot be completed before the end of the CAP, it must be deferred until the next super frame.

**Contention Free Period (CFP):** The CFP starts immediately after the end of the CAP and must complete before the start of the next beacon frame (if BO equals SO) or the end of the super frame. Transmissions are contention-free since they use reserved time slots (GTS) that must be previously allocated by the ZC or ZR of each cluster. All the GTSs that may be allocated by the Coordinator are located in the CFP and must occupy contiguous slots. The CFP may therefore grow or shrink depending on the total length of all GTSs. In beacon-enabled mode, each Coordinator defines a superframe structure Figure 1 which is constructed based on: The Beacon Interval (BI), which defines the time between two consecutive beacon frames. The Superframe Duration (SD), which defines the active portion in the BI, and is divided into 16 equally-sized time slots, during which frame transmissions are allowed. Optionally, an inactive period is defined if  $BI > SD$ . During the inactive period (if it exists), all nodes may enter in a sleep mode (to save energy). BI and SD are determined by two parameters, the Beacon Order (BO) and the Superframe Order (SO), respectively.  $aBaseSuperframeDuration = 15.36$  ms (assuming 250 kbps in the 2.4 GHz frequency band) denotes the minimum duration of the superframe, corresponding to  $SO=0$ . As depicted in Figure 3, low duty cycles can be configured by setting small values of the SO as compared to BO, resulting in greater sleep (inactive) periods. In ZigBee Cluster-Tree networks, each cluster can have different and dynamically adaptable duty cycles. This feature is particularly interesting for WSN applications, where energy consumption and network lifetime are main concerns. Additionally, the Guaranteed Time Slot (GTS) mechanism is quite attractive for time-sensitive WSNs, since it is possible to guarantee end-to-end message delay bounds both in Star and Cluster-Tree topologies.

### UWB CHANNEL AND DIVERSITY ANALYSIS FOR MULTIBAND OFDM

The UWB channel model developed under IEEE 802.15 [3] is a stochastic time-domain model. In this

section, we consider a stochastic frequency-domain description, i.e., we include transmitter IFFT and receiver FFT into the channel definition and consider realizations of  $H$ . In doing so, we intend to (a) extract the channel parameters relevant for the performance of OFDM-based UWB systems, (b) Examine whether the Multiband OFDM proposal is adequate to exploit the channel characteristics, (c) quantify the impact of the different UWB channel types on system performance and (d) possibly enable a classification of the UWB channel model into more standard channel models used in communication theory. From above analysis

we observe that the OFDM transmit signal experiences a frequency non-selective fading channel with fading along the frequency axis. Thereby, the outer lognormal shadowing term is irrelevant for the fading characteristics as it affects all tones equally. Hence, the lognormal shadowing term is omitted in the following considerations. Denoting the lognormal term by  $G$ , we obtain the corresponding normalized frequency-domain fading coefficients as

$$H_i^n = H_i/G \tag{1}$$

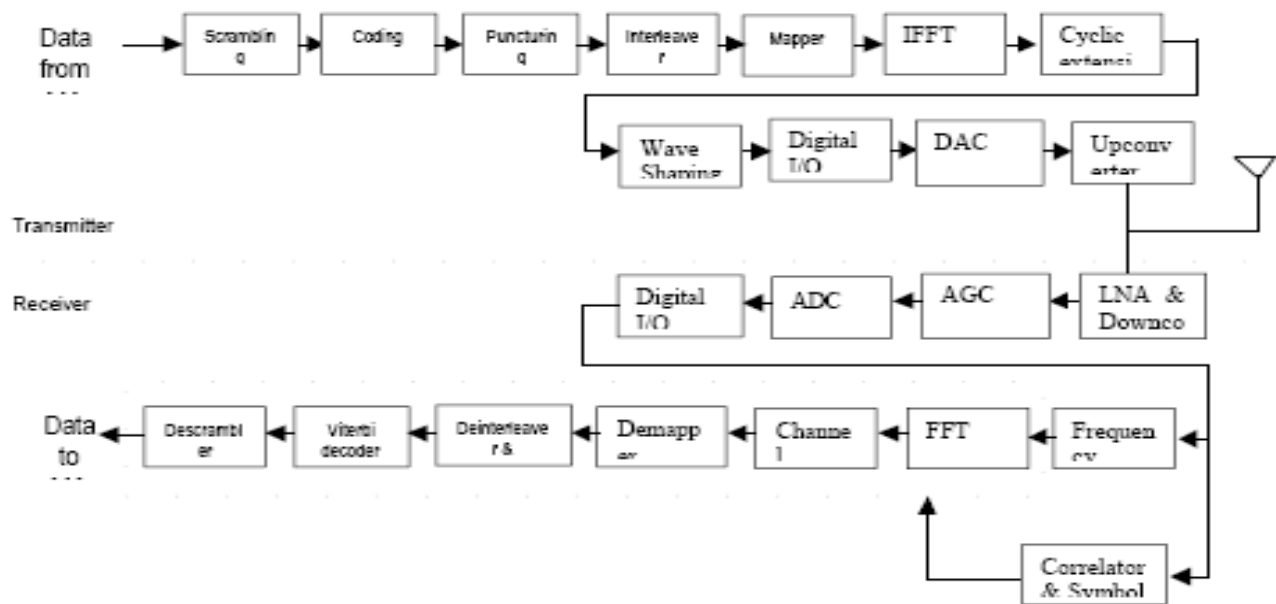


Figure 2: Block diagram of Multiband OFDM transmission system

**Marginal Distribution**

The first parameter of interest is the marginal distribution of  $H_i^n$ , i.e., the probability density function (pdf)  $p(H_i^n)$ . First, we note that the frequency-domain coefficient  $H_i^n$  is a zero mean random variable since the time-domain multipath components are zero mean quantities. Furthermore, we have observed that  $H_i^n$  is, in good approximation, circularly symmetric complex Gaussian distributed, which is explained by the fact that  $H_i^n$  results from the superposition of many time-domain multipath components. Since these multipath components are mutually statistically independent, the variance of  $H_i^n$  is independent of the tone index  $i$ . Figure.3 shows measurements of the pdfs  $p(|H_i^n|)$  of the magnitude frequency-domain gain  $|H_i^n|$  for the different channel models CM1-CM4, obtained from 10000 independent realizations of channel model. As can be seen, the experimental distributions agree well

with the exact Rayleigh distribution of equal variance, which is in accordance with the statements above. We note that similar conclusions regarding the frequency-domain gains were obtained independently in [9].

**Correlation**

The findings in the previous section indicate that the OFDM signal effectively experiences a (classical) frequency non-selective Rayleigh fading channel (along the OFDM subcarriers). Therefore, knowledge of the second-order channel statistics, i.e., the correlation between different fading coefficients  $H_i^n$  and  $H_j^n$ ,  $i \neq j$ , is important for the design and assessment of diversity techniques such as coding, interleaving, and frequency hopping, which are envisioned in the Multiband OFDM system. Since coding is performed over all bands, we consider all 3 bands jointly. As an appropriate figure of merit we

examine the ordered eigenvalues of the  $3-N \times 3-N$  correlation matrix  $R_{H^n H^n}$  of  $H^n = [H^n_1 \dots H^n_{3-N}]^T$ . Figure.4 shows the first 40 ordered eigenvalues (every second from 1<sup>st</sup> to 21<sup>st</sup>, and the 30<sup>th</sup> and 40<sup>th</sup>) of the measured  $R_{H^n H^n}$ , which has been obtained from averaging over 1000 channel realizations, as a function of the total employed signal bandwidth. We only show results for channel models CM1 and CM3, which constitute the two extreme cases as the corresponding impulse responses have the least (CM1) and most (CM3) independent multipath components. The respective curve for model CM2 lies in between those for CM1 and CM3. From Figure.4 we infer the following conclusions:

- (i) By increasing the bandwidth of the OFDM signal the diversity order of the equivalent frequency domain channel, i.e., the number of the significant non-zero eigen values of  $R_{H^n H^n}$ , is improved, since, generally, more time-domain multipath components are resolved. However, a 1500 MHz total bandwidth provides already  $\geq 40$  (CM3) and  $\geq 30$  (CM1) strong diversity branches. This indicates that the 528 MHz bandwidth and 3-band frequency hopping of Multiband OFDM is a favorable compromise between complexity and available diversity.
- (ii) Since the system, comprising the convolutional code with free distance  $\leq 15$  (depending on the puncturing) and spreading factor 1, 2, and 4, can at best exploit diversities of order 15, 30 and 60, respectively, bandwidths of more than 500 MHz per band would only be beneficial for the lowest data-rate modes, and then only for very low error rates. Similar considerations apply to concatenated codes, which do not exceed convolutional codes with spreading in terms of free distance.
- (iii) Though CM3 provides higher diversity order than CM1, the latter appears advantageous for high data-rate modes with code puncturing due to its larger first ordered eigenvalues.

In summary, we conclude that, given a particular realization of the lognormal shadowing term, the equivalent frequency-domain channel  $H$  is well approximated by a Rayleigh fading channel with relatively high “fading rate”, which increases from CM1 to CM3.

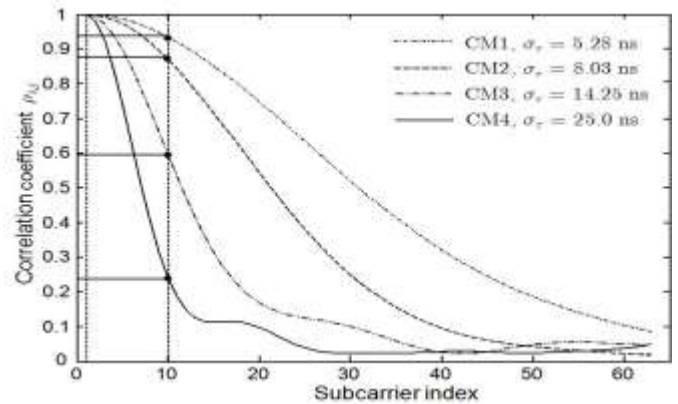


Fig.3. Distributions of normalized channel magnitude /  $H_i^n$  for channel types CM1-CM4. Rayleigh distribution with same variance.

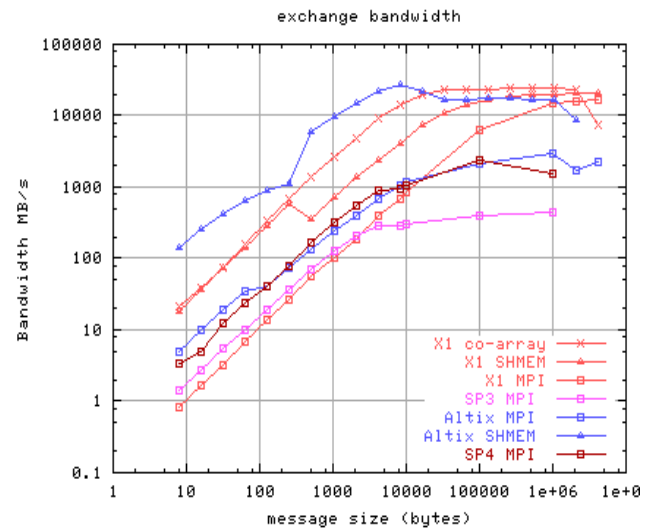


Figure.4 First ordered eigenvalues of the correlation matrix  $R_{H^n H^n}$

**Proposed methodology**

In this work we are working on the physical layer of network architecture in which we are trying to increase the error rate performance of the system by implementing multiple transmitters instead of single transmitter in existing system. We are replacing the AES Encryption method from ECC 160 as of recent research has done. The system design and simulation has been done on MATLAB 2011b environment. The algorithm of simulation procedure is given.

**SIMULATION RESULTS**

The simulation has been done with the MATLAB R2011b environment. During simulation we are calculating the Bit Error Rate for multiple transmitters using different iterations. We have also done analysis on five factors of PHY layer to support our research to

enhance the performance of ZigBee based Wireless Sensor Network. The vital role of MISO system in various applications and we implement the efficient MISO approach in MATLAB for ZigBee wireless technology also got the resourceful improvement in various parameters which are given below:

1. Reduced Bit Error Rate against Signal to Noise Ratio.
2. Capacity of ZigBee MISO System.
3. Battery Life Compression.
4. Performance of Probability of Error with various digital modulation techniques.
5. Data Rate
6. Power spectrum Density.

From above all the experiments it is clear that the “Green” & “Red” characteristics are showing better results of Bit Error Rate for lower values of SNR, which are for two and three transmitters respectively. Now if we use more than one transmitter instead of one (existing system) then the performance of Zigbee

(IEEE 802.15.4) system will improve. These results are based on simulation experiments and may vary during practical implementations in the actual conditions.

The Error Probability of Zigbee System shown in figure.6 for various digital modulation techniques. Digital modulation techniques are gives different performance with ZigBee. Speed (or data rate) and distance (or range) are inversely proportional. That is, other things being equal, a higher data rate system will not transmit as far as a lower data rate system. Radio frequency (RF) signals of a given carrier frequency, such as 2.4 gigahertz (GHz), lose power as they propagate. Called path loss, this is similar to the way a sound is softer the farther it is from the source. Path loss in decibels (dB) increases with the square of the distance and is relatively easy to estimate when the path is unobstructed. The free space loss equation at 2.4 GHz is simply this: path loss in dB = 40 dB + 20 log (distance in meters).

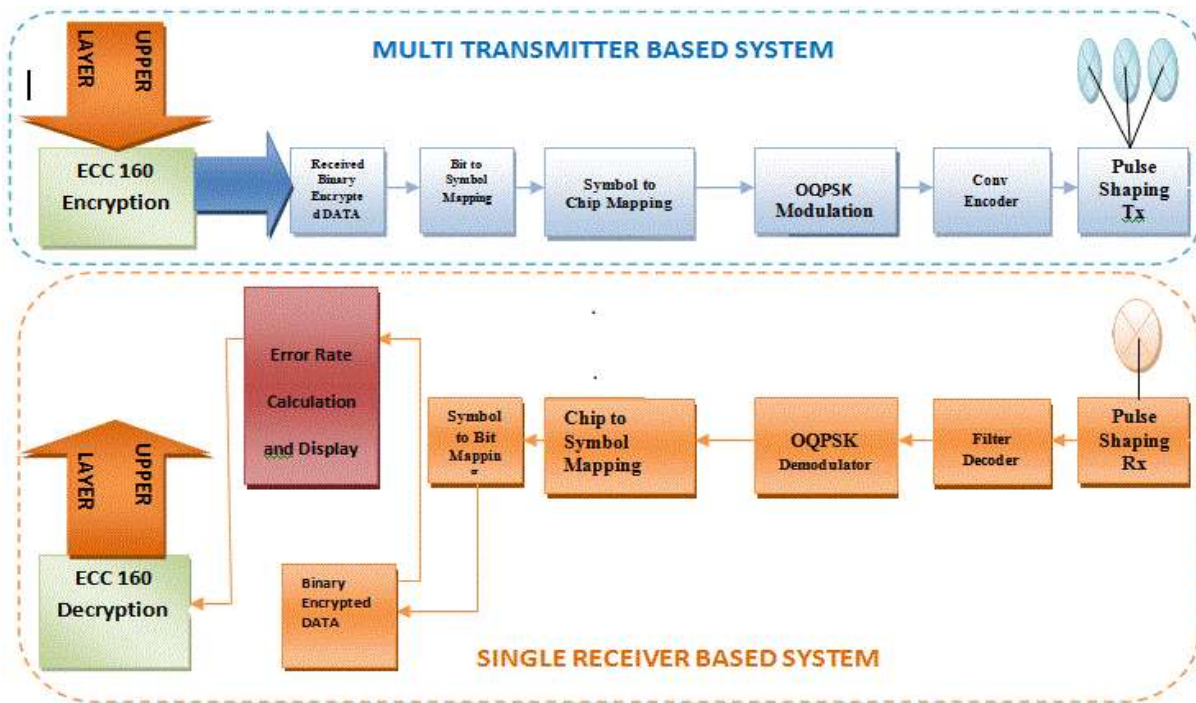
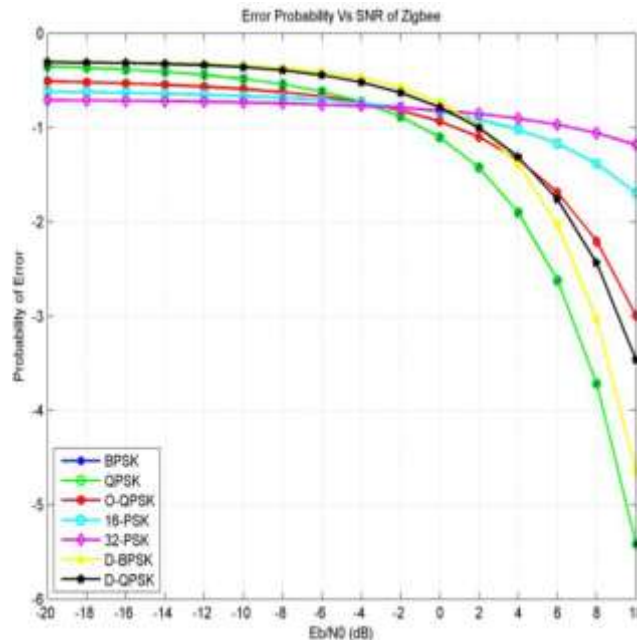


Figure.5 MISO & ECC 160 Encryption Based ZigBee Block Diagram for Proposed Model



**Figure.6 Performance of Probability of Error with Various Digital Modulation Techniques of ZigBee System**

In this Section, we study Turbo, RA, and convolutional coding without bit-loading. We examine channel CM1 with four different transmission modes with data rates of 80, 160, 320, and 480 Mbps corresponding to 0.25, 0.50, 1.00, and 1.50 bit/symbol, respectively. In the simulations, detection is performed with perfect CSI as well as with LSE channel estimation using  $\eta = 0.125$ . We then turn to the performance of systems. Based on the results of the information-theoretic analysis, we restrict our attention to rates  $\geq 1.00$  bit/symbol, where we expect loading algorithms to yield performance gains. We concentrate on Turbo and convolutional codes for this section. The simulation results presented in these two sections are the worst-case  $10 \log_{10}(\bar{E}_s/N_0)$  values required to achieve  $\text{BER} \leq 10^{-5}$  for the best 90% of channel realizations over a set of 100 channels (i.e. they are simulation results corresponding to 10% outage). We briefly summarize the power efficiency gains and attendant range improvements expected

from the application of the system extensions we have proposed.

Figure.7 shows SNR points when using convolutional codes (as in the Multiband OFDM proposed system), together with the corresponding 10% outage cutoff rate curves. We observe that the simulated SNR points are approximately 3 dB to 4 dB from the cutoff-rate curves, which is reasonable for the channel model and coding schemes under consideration. These results (a) justify the relevance of the information theoretic measure and (b) confirm the coding approach used in Multiband OFDM. More specifically, the diversity provided by the UWB channel is effectively exploited by the chosen convolutional coding and interleaving scheme. Furthermore, the system with LSE channel estimation performs within 0.5–0.7 dB of the perfect CSI case as was expected from the cutoff-rate analysis.

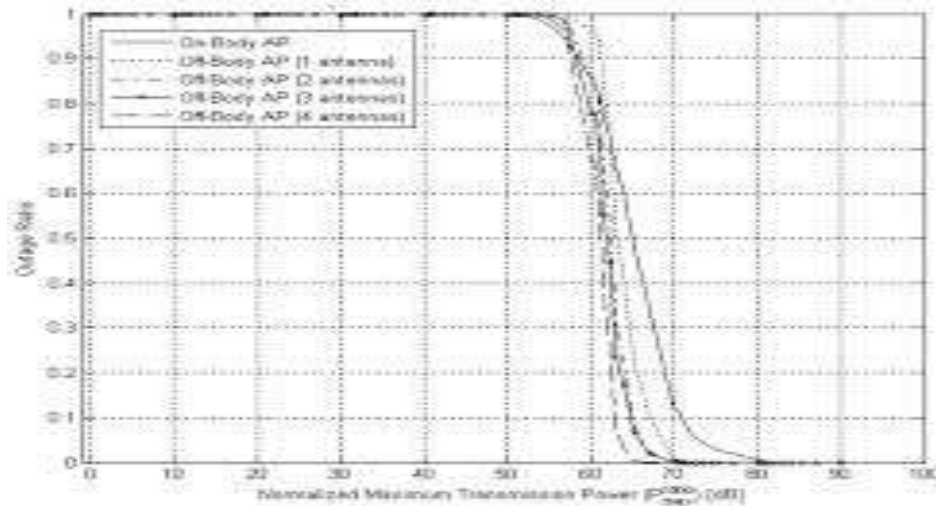


Figure.7.  $10 \log_{10}(\bar{E}_s/N_0)$  required to achieve  $BER \leq 10^{-5}$  for the 90% best channel realizations using convolutional codes. For comparison: 10% outage cutoff rate. Channel model CMI and LSE channel estimation.

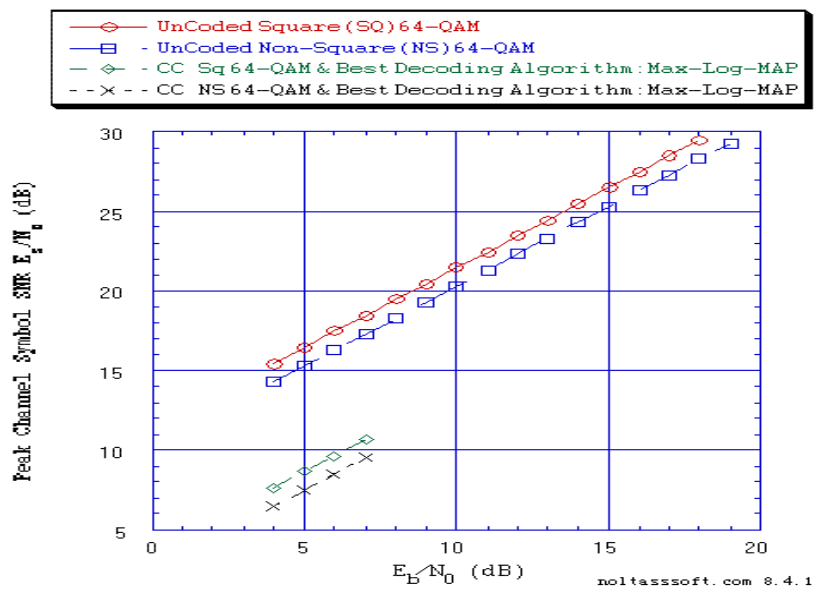


Figure.8.  $10 \log_{10}(\bar{E}_s/N_0)$  required to achieve  $BER \leq 10^{-5}$  for the 90% best channel realizations using Turbo Codes, RA codes, and convolutional codes. For comparison: 10% outage capacity and cutoff rate. Channel model CMI and perfect CSI.

We next consider the Turbo and RA coding schemes. Figure.8 shows the simulation results for Turbo and RA codes on channel CMI with perfect CSI, as well as the convolutional code results for comparison. We also show the corresponding 10% outage capacity and cutoff rate curves. Turbo codes give a performance gain of up to 5 dB over convolutional codes, and perform within 2.5 dB of the channel capacity, depending on the rate. At rates of 0.25 and 0.50 bit/symbol, Turbo code inter-leaver sizes compatible with the channel inter-leaver design of the Multiband OFDM proposal (the “std” points) incur a performance

penalty of 1–2 dB compared with the longer block length (“K=600”) points. Repeat accumulate codes have a performance roughly 1 dB worse than the long block-length Turbo codes, but the RA codes are both (a) compatible with the Multiband OFDM channel interleaver, and (b) less complex to decode. They are thus a good candidate for low-rate Multiband OFDM transmission.

### CONCLUSION

In this paper, we have shown that the UWB channel model developed under IEEE 802.15 is seen by



OFDM systems in the frequency domain as Rayleigh fading with additional shadowing. The 528 MHz signal bandwidth chosen for Multiband OFDM essentially captures the diversity provided by the UWB channel. As a result, we have found that the information-theoretic limits of the UWB channel are similar to those of a perfectly interleaved Rayleigh fading channel with shadowing. The BICM-OFDM scheme proposed for Multiband OFDM performs close to the outage cutoff-rate measure and is thus well suited to exploit the available diversity. The application of stronger coding, such as Turbo codes or Repeat-Accumulate codes, improves power efficiency by up to 5 dB, depending on the data rate. Bit-loading algorithms provide additional performance gains for high data rates, and a simple clustering scheme allows for reduced-rate feedback of loading information depending on the channel conditions and required power efficiency. From the Simulation results, the existing ZigBee system with 2.4 GHz band and with O-QPSK modulation works significantly with low power operations but there is always a need some improvement in the system, so here we have tried to reduce the Bit Error Rate and taken an analysis on five factors of ZigBee system and tried to reduce the power consumption using ECC 160 security algorithm also the Power of the system which will be the revolution in the field of 802.15.4. Here we have increased the number of transmitters which greatly reduces the error rate of the existing system. Here we simulate system up to three transmitters but in future with the developments in the antenna technology we can increase more transmitters as our ease. The future of our proposed work will be the lowest power consumption Personal Area Network (PAN) for information sharing and network access.

## REFERENCES

1. W. P. Siriwongpairat, Z. Han, and K. R. Liu, "Energy-Efficient Resource Allocation for

- Multiband UWB Communication Systems," in Proc. IEEE Wireless Comm. & Networking Conf. (WCNC), vol. 2, Mar. 2005, pp. 813–818.
2. J. Stankovic, I. Lee, A. Mok, R. Rajkumar, "Opportunities and Obligations for Physical Computing Systems", in IEEE Computer, Volume 38, Nov, 2005.
3. A. F. Molisch, J. R. Foerster, and M. Pendergrass, "Channel Models for Ultrawideband Personal Area Networks," IEEE Wireless Commun. Mag., vol. 10, no. 6, pp. 14–21, Dec. 2003.
4. A. Saleh and R. Valenzuela, "A Statistical Model for Indoor Multipath Propagation," IEEE J. Select. Areas Commun., vol. SAC-5, no. 2, pp. 128–137, Feb. 1987.
5. J. G. Proakis, Digital Communications, 4th ed. New York: McGraw-Hill, 2001.
6. G. Caire, G. Taricco, and E. Biglieri, "Bit-Interleaved Coded Modulation," IEEE Trans. Inform. Theory, vol. 44, no. 3, pp. 927–946, May 1998.
7. J. Hagenauer, E. Offer, and L. Papke, "Iterative Decoding of Binary Block and Convolutional Codes," IEEE Trans. Inform. Theory, vol. 42, no. 2, pp. 429–445, Mar. 1996.
8. D. J. MacKay, "Gallager Codes — Recent Results," University of Cambridge, Tech. Rep., [Online] <http://www.inference.phy.cam.ac.uk/mackay/>.
9. M.-O. Wessman, A. Svensson, and E. Agrell, "Frequency Diversity Performance of Coded Multiband-OFDM Systems on IEEE UWB Channels," in Proc. IEEE Vehic. Tech. Conf., Fall (VTC), vol. 2, Sept. 2004, pp. 1197–1201.